Modeling pressure-driven assembly of polymer coated nanoparticles

Cite as: AIP Conference Proceedings **1979**, 090007 (2018); https://doi.org/10.1063/1.5044864
Published Online: 03 July 2018

J. Matthew D. Lane, K. Michael Salerno, Ishan Srivastava, Gary S. Grest, and Hongyou Fan

Modeling Pressure-driven Assembly of Polymer Coated Nanoparticles

J. Matthew D. Lane[1,a)], K. Michael Salerno[2], Ishan Srivastava[1], Gary S. Grest[1] and Hongyou Fan[1,3]

[1]*Sandia National Laboratories, Albuquerque, NM 87185, USA*
[2]*U.S. Naval Research Laboratory, Washington, D.C. 20375, USA*
[3]*Department of Chemical and Biological Engineering, University of New Mexico, Albuquerque, NM 87106, USA*

[a)]Corresponding author: jlane@sandia.gov

Abstract. High-pressure experiments have successfully produced a variety of gold nanostructures by compressing polymer coated spherical nanoparticles. We apply atomistic simulation to understand the role of the soft polymer response in determining the pressure-driven assembly of gold nanostructures. Quasi-isentropic experiments have shown that 1D, 2D and 3D nanostructures can be formed and recovered from dynamic compression of fcc superlattices of alkanethiol-coated gold nanocrystals on Sandia's Veloce pulsed power accelerator. Molecular modeling has shown that the dimensionality of the final structures depends on the orientation of the superlattice and the uniaxial loading. We describe the role of coating ligand binding strength, on ligand migration and deformation processes during pressure-driven coalescence of the cores into permanent nanowires, nanosheets and 3D structures.

INTRODUCTION

Nanostructured gold and gold nanoparticle arrays have many applications – such as sensing, nanoelectronics and photonic materials – due to their unique optical properties, which can be tuned by altering the structure geometry. Polymer coatings are often employed to prevent aggregation, and control nanoparticle-nanoparticle separation distance. These coated nanoparticles can self-assemble into ordered 2D or 3D geometries. The assembly of these structures has been studied experimentally [1, 2, 3] and computationally [4, 5, 6, 7]. Fan and co-workers [3, 8] have used quasi-static high-pressure to control the ordering and, at high enough pressures, to form sintered nanowires and 3D extended structures. The dynamics of this pressure-driven process and its sensitivity to the nanoparticle core and coating properties is a rich area of study.

More recently, Li *et al.* [9] have demonstrated pressure-driven assembly on nanosecond timescales, using Sandia's Veloce pulsed power accelerator, to isentropically compress these superlattices of hybrid soft and hard matter. This innovative nanofabrication process provides a high-rate method for synthesizing nanorods, nanowires, nanosheets, and bulk 3D structures. A key goal in this ongoing research is to reduce the sintering threshold pressure, and improve process efficiency.

To successfully exploit nanostructured materials and nanoparticle composites, it is critical to understand how variations in the nanoparticle size, shape, and coating affect the mechanical properties of the material, including how these materials respond and ultimately coalesce in compression. Atomistic modeling can be used to quickly and inexpensively probe the sensitivity to these parameters. Past successes have demonstrated how atomistic modeling can be used with Sandia's unique experimental capability in extreme pressure regimes to greatly improved understanding of the molecular processes involved in extreme compression of soft materials [10, 11].

METHODOLOGY

We use classical molecular dynamics simulation to study high-rate compression of gold nanoparticles, coated with short-chain polymers. Sandia's LAMMPS [12] code was used with an all-atom model. The hydrocarbon interactions

Shock Compression of Condensed Matter - 2017
AIP Conf. Proc. 1979, 090007-1–090007-5; https://doi.org/10.1063/1.5044864
Published by AIP Publishing. 978-0-7354-1693-2/$30.00

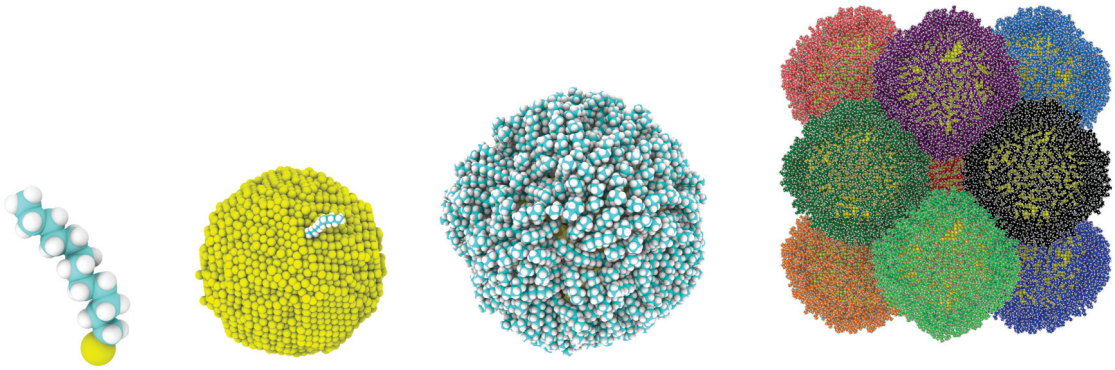

FIGURE 1. Systems of polymer-coated nanoparticles are constructed with hierarchical building blocks. a) short-chain polymers are constructed with appropriate bonds, angles and dihedrals. b) a single chain is grafted to a 6 nm diameter fcc gold nanoparticle. c) A fully-coated gold nanoparticle. d) a collection of coated nanoparticles forming an fcc superlattice (colored to emphasize individual nanoparticles).

were modeled using the OPLS force field [13, 14] modified with an updated dihedral potential [15] and with non-bonded interactions using an exponential-6 form [16]. Gold atoms were modeled using the embedded atom method [17]. The gold-sulfur interactions were modeled with a Morse potential with parameterizations from Luedtke and Landman [18] and Henz *et al.* [19]. Each S-Au interaction gives a different binding strength, i.e. 9.2 kcal/mol for the former and a weaker 2.18 kcal/mol for the latter. A 1.0 fs timestep was used during ambient equilibration, and decreased to 0.2 fs during compression. Long-range Coulomb corrections were included using the particle-particle-particle-mesh PPPM method [20].

The hierarchical construction of the hybrid soft/hard system is depicted in Figure 1. Nanoparticle cores were cut from fcc gold crystal to form 5.9 nm diameter spheres. The coating consisted of dodecanethiol, $S[CH_2]_{11}CH_3$, ligands placed at full coverage (4.7 chains per nm^2) on the gold core. Preparation details are given in Ref. [21]. 515 hydrocarbon chains were physisorbed on each core's surface, and were able to move over the surface or even to detach under mechanical stresses. These coated nanoparticles were then assembled into an fcc superlattice with a lattice constant of 10.6 nm, giving a core-core center spacing of ~7.6 nm. The systems were equilibrated at zero pressure for 1 ns before being rotated and subjected to dynamic loading. To distinguish the lattice of nanoparticle from the lattice of gold atoms within each core, we refer to the larger lattice of nanoparticles as a superlattice.

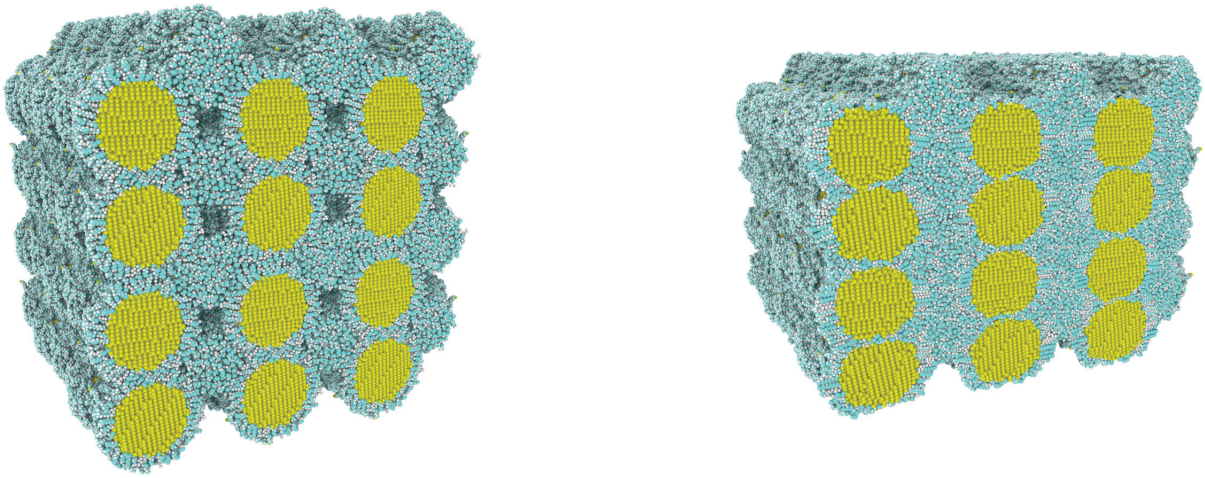

FIGURE 2. Initial (left) and final (right) snapshots of uniaxial compression to 15 GPa along the [110] direction of the fcc nanoparticle superlattice.

Dynamic compression was modeled using a constant-stress Hugoniostat approach [22] to simulate uniaxial compression. Figure 2 shows representative states before and after compression to 15 GPa. While the experimental compression was done quasi-isentropically to minimize heating/melting of the cores, our simulations used a shock compression in order to minimize computation cost. This methodology was later confirmed with identical results from an isothermal ramp compression. Heating and melt of the gold cores, while important in the experiments, were found to play little role on the hundred picosecond timescales of these simulations. The Hugoniostat employs homogeneous compression coupled with a thermostat which constrains the temperature to enforce the Rankine-Hugoniot relations. The Hugoniostat approach is less costly because it does not require large systems, since there is no explicit wave propagation.

RESULTS

Representative slices of nearest-neighbor clusters are shown in Figure 3 for the initial and final configurations of the superlattice strained along its [100], [110] and [111] directions. In the undeformed fcc superlattice, each nanoparticle has 12 neighbors. The various slices show how these original 12 neighbors respond to compression along different orientations. We see that compression along [110], [111] and [100], results in 2, 6 and 8 nearest neighbors, respectively. The neighbor analysis and images illustrate the formation of wires in the [110] case. The [111] analysis is consistent with either three-dimensional, or possibly planar structures (i.e. six nearest neighbors is consistent with an in-plane hexagonal structure). The compression along [100] appears from the images to give three-dimensional structures, but the nearest-neighbor number of 8 indicates a three-dimensional structure with reduced symmetry from a perfect fcc

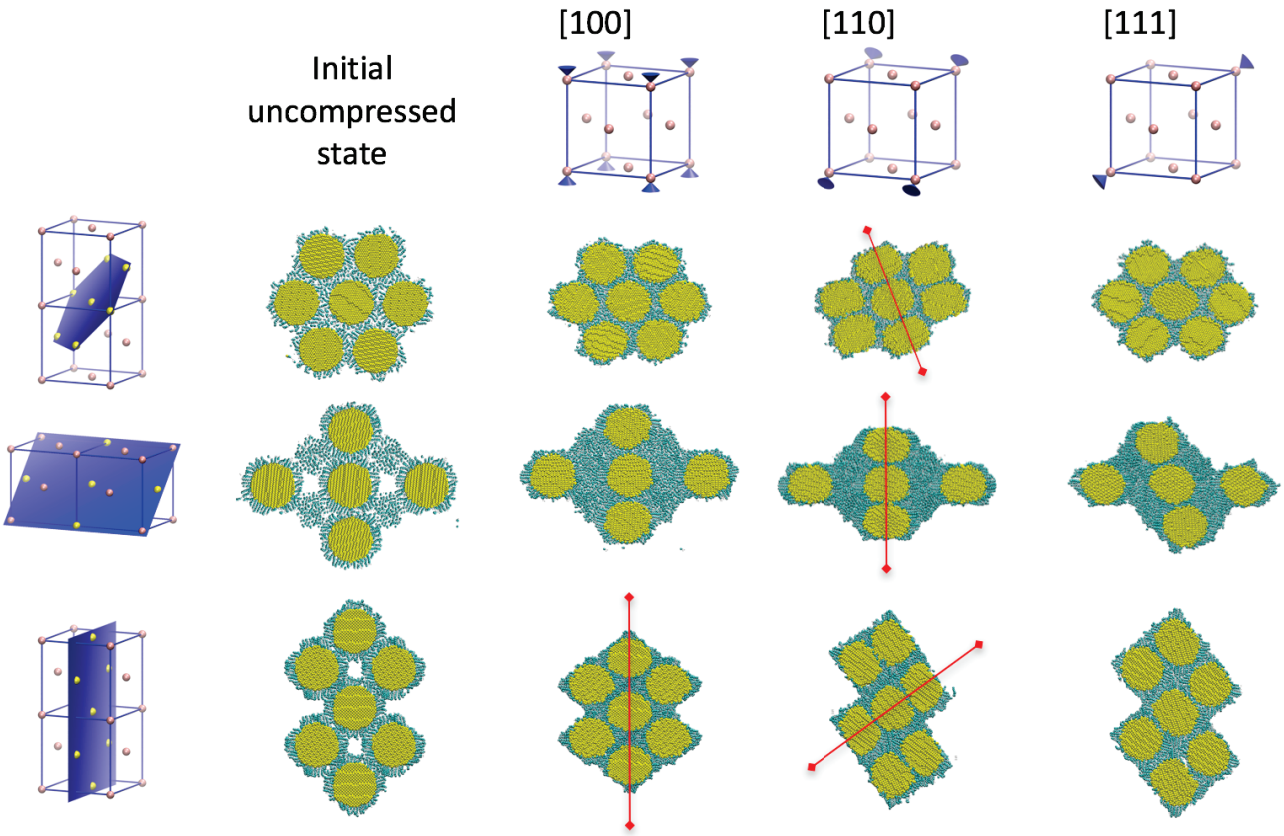

FIGURE 3. Various slices through the simulation box showing nearest-neighbor clusters from the fcc superlattice of gold nanoparticles and their polymer coatings. Images show uncompressed systems in addition to compression along three orthogonal lattice directions. If the compression direction falls in the plane of the slice, it is shown by a red arrow. Modified with permission following Li *et al.* [9] and Nature Publishing Group, under the Creative Commons Public License 4.0.

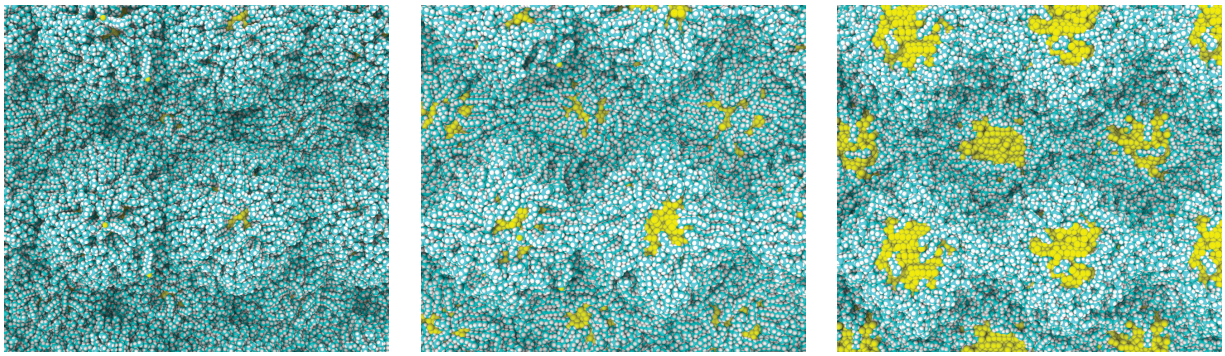

FIGURE 4. End-on views of the contact between adjacent nanoparticles, where the direction of [110] compression direction comes out of the page. The original uncompressed system is on the left. The 9.2 kcal/mol S-Au binding energy system is in the center. The 2.18 kcal/mol S-Au binding energy is on the right.

lattice. It is interesting to note the significant localization of the deformation in the soft ligand chains.

Figure 4 shows the behavior of the ligands which are initially trapped between coalescing cores. At the sintering points between adjacent cores, ligands can be seen being pushed out from the regions between the nanoparticle cores. The chains, however, do not leave the core surface, but simply compact on the remaining particle surface. On timescales longer than these simulations, one would expect that some number of ligand chains would ultimately be released.

Even experimentally, there is some uncertainty in the S-Au binding energy and it was unclear what effect the difference would have on the sintering process. So, we selected two potentials which had binding energies of 9.2 kcal/mol from Luedtke and Landman [18] and 2.18 kcal/mol from Henz *et al.* [19]. Figures 4 and 5 show that the binding energy has a significant effect on the final sinter separation, and in the degree to which chains are successfully cleared from the approaching cores. In Figure 5, one observes that there is greater transverse displacement of the polymer chains for the lower energy binding case. This may be the result of a lower resistance to pull-off in the weaker binding case, which allows the sulfur to pull away from the surface rather than being pinned between the nanoparticles. The details of this mechanism deserves a more thorough investigation.

CONCLUSIONS

In conclusion, we have studied the response of soft/hard hybrid systems of polymer coated nanoparticles to investigate the role of polymer properties to the overall compression response, and sintering. We find that the final nanostructural geometries produced depend on the alignment between the superlattice orientation and the loading direction. Compression along the [110] orientation led to wire formation, while compression along [111] led to a three-dimensional nanostructure. Compression along [100] led to either planar aggregation or three-dimensional structures. Further, we

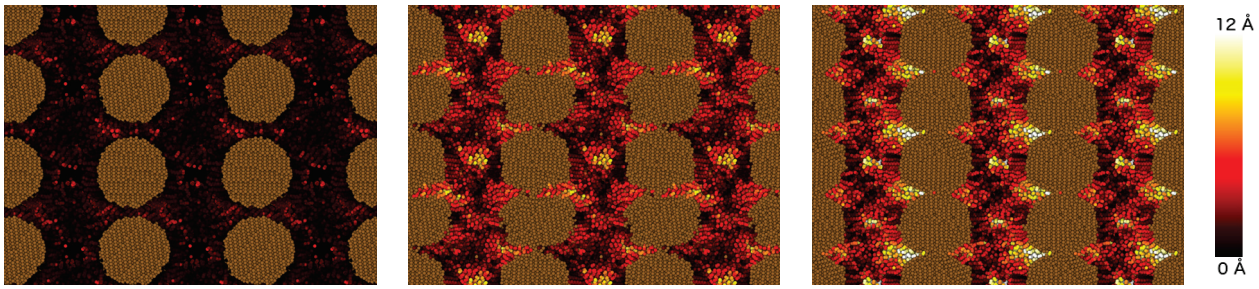

FIGURE 5. Slices through the system showing the [110] in the vertical, colored by horizontal displacement. The orginal uncompressed system is on the left. The 9.2 kcal/mol S-Au binding energy system is in the center. The 2.18 kcal/mol S-Au binding energy is on the right.

find that the degree of sintering is significantly affected by changes in the S-Au binding energy. While this is not an easily tunable experimental parameter for S-Au. It is effectively tunable by switching between Au and Ag cores. Lowering the binding energy seems to indicate that nanoparticle-nanoparticle sintering threshold pressures could be reduced. A similar analysis of the effect of chain length, and grafting density is ongoing and will be published elsewhere.

ACKNOWLEDGMENTS

This work was supported by the U.S. Department of Energy, Office of Basic Energy Sciences, Division of Materials Sciences and Engineering. Research was carried out, in part, at the Center for Integrated Nanotechnologies, a US Department of Energy, Office of Basic Energy Sciences user facility. Sandia National Laboratories is a multi-mission laboratory managed and operated by National Technology and Engineering Solutions of Sandia, LLC., a wholly owned subsidiary of Honeywell International, Inc., for the U.S. Department of Energy's National Nuclear Security Administration under contract DE-NA0003525.

REFERENCES

[1] T. P. Bigioni, L. Xiao-Min, T. T. Nguyen, E. I. Corwin, T. A. Witten, and H. M. Jaeger, Nature Mater. **5**, 265 (2006).
[2] J. He, P. Kanjanaboos, N. L. Frazer, A. Weis, X.-M. Lin, and H. M. Jaeger, Small **6**, 1449 (2010).
[3] H. Wu, F. Bai, Z. Sun, R. E. Haddad, D. M. Boye, Z. Wang, J. Y. Huang, and H. Fan, J. Am. Chem. Soc. **132**, 12826 (2010).
[4] J. M. D. Lane and G. S. Grest, Phys. Rev. Lett. **104**, 235501 (2010).
[5] J. M. D. Lane and G. S. Grest, Nanoscale **6**, 5132 (2014).
[6] K. M. Salerno, D. S. Bolintineanu, J. M. D. Lane, and G. S. Grest, Phys. Rev. Lett. **113**, 258301 (2014).
[7] W. Li, H. Fan, and J. Li, Nano Lett. **14**, 4951 (2014).
[8] B. Li, X. Wen, R. Li, Z. Wang, P. G. Clem, and H. Fan, Nature Commun. **5**, 4179 (2014).
[9] B. Li, K. Bian, J. M. D. Lane, K. M. Salerno, G. S. Grest, T. Ao, R. Hickman, J. Wise, Z. Wang, and H. Fan, Nature Commun. **8**, 14778 (2017).
[10] T. R. Mattsson, J. M. D. Lane, K. R. Cochrane, M. P. Desjarlais, A. P. Thompson, F. Pierce, and G. S. Grest, Phys. Rev. B **81**, 054103 (2010).
[11] S. Root, T. A. Haill, J. M. D. Lane, A. P. Thompson, G. S. Grest, D. G. Schroen, and T. R. Mattsson, J. Appl. Phys. **114**, 103502 (2013).
[12] S. Plimpton, J. Comp. Phys. **117**, p. 1 (1995),
LAMMPS code available at http://lammps.sandia.gov.
[13] W. L. Jorgensen, J. D. Madura, and C. J. Swenson, J. Am. Chem. Soc. **106**, 6638 (1984).
[14] W. L. Jorgensen, D. S. Maxwell, and J. Tirado-Rives, J. Am. Chem. Soc. **118**, 11225 (1996).
[15] S. W. Siu, K. Pluhackova, and R. A. Bockmann, J. Chem. Theory Comput. **8**, 1459 (2012).
[16] O. Borodin and G. D. Smith, J. Phys. Chem. B **110**, 6279 (2006).
[17] S. Foiles, M. Baskes, and M. Daw, Phys. Rev. B **33**, 7983 (1986).
[18] W. Luedtke and U. Landman, J. Phys. Chem. B **102**, 6566 (1998).
[19] B. J. Henz, T. Hawa, and M. R. Zachariah, Langmuir **24**, 773 (2008).
[20] R. W. Hockney and J. W. Eastwood, *Computer simulation using particles* (crc Press, 1988).
[21] K. M. Salerno, D. S. Bolintineanu, J. M. D. Lane, and G. S. Grest, Phys. Rev. E **91**, 062403 (2015).
[22] R. Ravelo, B. L. Holian, T. C. Germann, and P. S. Lomdahl, Phys. Rev. B **70**, 014103 (2004).